Am J Transl Res 2022;14(4):2331-2342
www.ajtr.org /ISSN:1943-8141/AJTR0138920

Original Article

LINC01272 activates epithelial-mesenchymal transition through miR-153-5p in Crohn's disease

Lin Fang, Mengcheng Hu, Fei Xia, Wenxia Bai

Department of Gastroenterology, The Affiliated Jiangning Hospital of Nanjing Medical University, Nanjing 211100, Jangsu, China

Received September 6, 2021; Accepted March 17, 2022; Epub April 15, 2022; Published April 30, 2022

Abstract: Objectives: Long noncoding RNAs (lncRNAs) have different functions in different diseases. There is little research on the functions of lncRNAs in Crohn's disease (CD). By using RNA-seq technology, we identified a lncRNA associated with Crohn's disease. However, the mechanism of lncRNA regulation remains unknown. This study aimed to determine the association of LINC01272 with epithelial cell-mesenchymal transition and the underlying mechanism in CD. Methods: RNA was detected by qRT-PCR. The interaction of protein and RNA was determined by RNA binding protein immunoprecipitation. Luciferase reporter assays were used to detect the targeted miRNA of LINC01272. Tissue fibrosis was observed by Masson and H&E staining. Protein expression was determined by western blotting and immunofluorescence. Results: LINC01272 was highly expressed in patients with CD. Knockdown of LINC01272 inhibited TGF-β1-induced epithelial-mesenchymal transition (EMT). Additionally, LINC01272 regulated TGF-β1-induced EMT through the miR-153-5p axis, and knockdown of LINC01272 inhibited EMT in CD mice *in vivo*. Conclusion: LINC01272 activated the epithelial-mesenchymal transition through miR-153-5p in CD.

Keywords: Crohn's disease, LINC01272, miR-153-5p, EMT

Introduction

CD is an unexplained intestinal inflammatory disease that occurs in any part of the gastrointestinal tract, but usually in the terminal ileum and right colon [1-5]. Both CD and chronic nonspecific ulcerative colitis are collectively referred to as inflammatory bowel disease (IBD). The clinical manifestations of this disease are abdominal pain, diarrhea, intestinal obstruction, and extraintestinal manifestations such as fever and nutritional disorders [6, 7]. The course of the disease is often protracted and recurrent, and it is not easy to cure. The common nosogenesis of CD includes genetic mutations, environmental factors, and personal immunity [8-10]. Under pathogenic conditions, intestinal mucosal cells undergo EMT, and epithelial cells lose their polarity and intercellular adhesion [11, 12]. Myofibroblasts with strong movement and migration ability also secrete large amounts of extracellular matrix (such as collagen-I and collagen-III). EMT has a dual effect on the formation of tissue fibrosis: (1) EMT increases the number of mesenchymal cells and matrix production; (2) EMT causes the loss of epithelial cells and increases tissue damage [13, 14]. During this process, the expression of epithelial cell markers such as E-cadherin is decreased, and the expression of mesenchymal cell markers such as smooth muscle agonist protein (α-SMA), N-cadherin (N cadherin), and fibronectin increases [15-18].

Noncoding RNA (ncRNA) is currently one of the most popular research topics in the field of biomedicine [19, 20]. Transcripts with a length of fewer than 200 nucleotides are called short noncoding RNAs, such as microRNAs (miRNAs), RNAs (PIWI-interacting RNAs, piRNAs), and small interfering RNAs (small interfering RNAs, siRNAs) [21, 22]. Another type of RNA that acts as a miRNA sponge is called long noncoding RNAs (lncRNAs). LncRNAs generally refer to RNAs greater than 200 nucleotides in length and they rarely participate in protein coding [23]. As competitive endogenous RNAs (ceRNAs), lncRNAs can combine with miRNAs, inhibit the effect of miRNAs on target genes and are located in the nucleus or cytoplasm [24]. Their

Table 1. Clinical characteristics of patients

Characteristics	Normal Control (n=30)	Crohn's Disease (n=30)
Gender		
male	17	18
female	13	12
Mean age, years ± SD	30.38±9.24	31.45±10.16
Mean duration of disease, years ± SD	-	
Disease distribution		
Ileal	-	6
Colonic	-	8
Ileo-colonic	-	15
Peri-ana	-	1
Medications		
Mesalamine	-	7
Antibiotics	-	9
Steroids	-	8
Immunomodulators	-	6

expression is tissue-specific and spatiotemporally specific. LINC01272, as a novel marker, has not been found in many studies.

In our study, the purpose was to probe the functions of LINC01272 in CD and its potential mechanism. We found that LINC01272 activated EMT by regulating miR-153-5p expression in CD. Our study will provide an experimental basis for CD treatment and offer therapeutic targets against CD.

Methods

Clinical samples

Samples were taken from CD patients with colonic and ileal inflammatory lesions. Normal tissue was taken from healthy subjects undergoing colonoscopy. All samples were obtained from the Affiliated Jiangning Hospital of Nanjing Medical University and General Hospital of Eastern Theater Command between October 2019 and October 2020. All participants signed informed consent forms. Our experiments were approved by the ethics community of the Affiliated Jiangning Hospital of Nanjing Medical University. The clinical characteristics of CD and control patients are presented in **Table 1**.

Cell culture and transfection

IEC-6 cells (ATCC, Manassas, VA) were cultured in DMEM containing 10% fetal bovine serum (FBS) at 5% CO_2 and 37°C. The shRNAs for LINC01272 and its corresponding scrambled siRNAs (sh-NC) were purchased from Hanbio (Shanghai, China). miRNA oligonucleotides, including miR-153-5p mimic, miR-153-5p inhibitor, NC mimic and NC inhibitor, were obtained from RiboBio (Guangzhou, China). Transient transfection was performed by using Lipofectamine 3000 (Invitrogen, Carlsbad, CA, USA) according to the manufacturer's protocol. Cells were harvested 48 h post-transfection for further experiments.

Establishment of CD mouse models

We used 2,4,6-trinitrobenzenesulfonic acid (TNBS) to construct a CD mouse model following a previous study [25]. Thirty female BALB/C mice were randomly divided into the control group (n=10), TNBS group (n=10), and TNBS+ sh-LINC01272 group (n=10). The control group was fed a conventional diet, and the latter two groups were fed TNBS (3.75 mg) to establish the CD model. Mice were shaved before the experiment and coated with TNBS 3.75 mg (dissolved in 48% ethanol). After fasting for 24 h, mice were narcotized using pentobarbital sodium on the 7th, 14th and 21st days after TNBS coating. The trocar was inserted into the colon with a 20 G trocar in the prone position, the top of which was approximately 4 cm away from the anus. An ethanol solution of 100 μl of TNBS was injected into the lumen in a relaxed manner immediately by a 1 ml syringe fixed with a trocar. In the third group, mice were injected intraperitoneally with 500 μL of sh-LINC01272. The blank control and the model group were treated with the same amount of saline. After the first treatment, the disease activity index (DAI) scores were recorded according to a previous report [26].

qRT-PCR analysis

TRIzol was used to isolate RNA from cells or tissues. After the RNA was completely dissolved, the 5× PrimeScript® RT Master Mix Kit was used for reverse transcription (10 μL). qRT-

Table 2. Primer sequences used for qRT-PCR

Genes		Primer sequences (5'-3')
Hsa-LINC01272	Forward	CCAAGGTCACGCAGCACAGTC
	Reverse	GCAGAGATGAGCAGCAGTGGTG
Has-GAPDH	Forward	GGTGAAGGTCGGAGTCAACG
	Reverse	CAAAGTTGTCATGGATGHACC
Hsa-miR-153-3p	Forward	GCCGGGCTTGCATAGTCACAA
Has-U6	Forward	CGCTTCGGCAGCACATATAC
Rno-miR-153-3p	Forward	TTGCATAGTCACAAAAGTGATCG
	Reverse	GTGTCGTGGAGTCGGCAA
Rno-E-cadherin	Forward	GGTGAATTTTTAGTTAATTAGCGGTAC
	Reverse	CATAACTAACCGAAAACGCCG
Rno-collagen I	Forward	TGCTGCCTTTTCTGTTCCTT
	Reverse	AAGGTGCTGGGTAGGGAAGT
Rno-collagen III	Forward	GAGGAATGGGTGGCTATCCG
	Reverse	TTGCGTCCATCAAAGCCTCT
Rno-N-cadherin	Forward	GTGCCATTAGCCAAGGGAATTCAGC
	Reverse	GCGTTCCTGTTCCACTCATAGGAGG
Rno-CK	Forward	CACAAGAAGACACTACGAATC
	Reverse	-ACGACTATGAGGACGAAGA
Rno-α-SMA	Forward	TAGCGAGCATCACTGACA
	Reverse	AACATAGAGCCAAGCAACA
Rno-Fibronectin	Forward	CGAAATCACAGCCAGTAG
	Reverse	ATCACATCCACACGGTAG
Rno-GAPDH	Forward	ACTCACTCTTCTACCTTTGATGCT
	Reverse	TGTTGCTGTAGCCAAATTCA

PCR was carried out by SYBR Premix Ex Taq TM (Takara, Otsu, Japan) on a StepOnePlus™ Real-Time PCR System (Thermo Fisher Scientific). The PCR conditions were as follows: 94°C for 5 min, followed by 40 cycles at 94°C for 30 s, 55°C for 30 s, and 72°C for 60 s. The primers for qRT-PCR are shown in **Table 2**.

Western blot

A bicinchoninic acid (BCA) kit (Wuhan Bost Biotechnology Company, Hubei, China) was used to extract the total proteins required for the experiment and detect their concentrations. Then, 30 mg/well loading buffer was added to the extracted proteins and boiled in a 95°C water bath for 5 min. After that, the proteins were first separated by 10% polyacrylamide gel electrophoresis (Wuhan Bode Biotechnology, Hubei, China) and transferred to PVDF transmembranes (Millipore). Finally, the transferred transmembrane was placed in skim milk for 1 h. These bands were incubated with primary antibodies (1:1000, Abcam, MA, USA) at 4°C overnight. Subsequently, these bands were treated with the indicated secondary antibodies for 1-2 h. A dual-color infrared fluorescence scanning imaging system (Odyssey, Licor, NE, USA) was used to capture images, and then ImageJ 1.52v imaging analysis software (NIH, Bethesda, MD, USA) was used for analysis.

Immunofluorescence

IEC-6 cells were cultured in immunofluorescence-specific plates. Cells were washed using PBS and fixed in 4% paraformaldehyde for 20 min. Then, the cells were blocked with 0.1% BSA for 30 min at 23°C. Next, the cells were incubated with primary rabbit anti-collagen I (1:100 dilution) or rabbit anti-collagen III antibodies (1:100) overnight at 4°C. Alexa 555 secondary antibodies (Molecular Probes, Thermo Fisher Scientific, USA) and DAPI were used to incubate the cells. The cells were observed under a fluorescence microscope (Keyence, Ōsaka, Japan).

RNA binding protein immunoprecipitation

The RIP experiment was carried out with the Magna RIP Kit (Magna, ON, CAN). Briefly, the lysed cells were treated with RIP buffer solution, and the magnetic beads were labeled using anti-Ago2 or IgG. The abundance of LINC01272 and miR-153-5p was verified by qRT-PCR.

Luciferase reporter assays

The promoter region of LINC01272 was cloned by PCR and inserted into the pGL3-LINC01272-WT and MUT plasmids through enzyme digestion to construct a Renilla luciferase vector. For the promoter region of LINC01272, the forward primer was "CGACUGACGCCG", and the reverse primer was "UCGACAUCGA". The miR-153-5p plasmids were cotransfected with pGL3-LINC01272 WT-Renilla luciferase vector or pGL3-LINC01272 MUT-Renilla luciferase vector into IEC-6 cells by Lipofectamine 2000 (Invitrogen). After the transfection plasmid

was added to cells by Lipofectamine 3000 (Invitrogen) for 48 h, the Renilla luciferase in cell lysate was assessed by the dual-luciferase reporter assay system (BEST, Nanjing, China).

Masson staining

The tissue sections were stained with Masson's reagent according to the following procedures: (i) fixed in Bouin's or Zenker's liquor overnight, (ii) washed in running water until the yellow color faded and rinsed in distilled water twice, (iii) stained with hematoxylin for 5 min, (iv) placed in 0.5% hydrochloric acid in 70% alcohol for 5 s, (v) washed for 30 s in running tap water and rinsed in distilled water twice, (vi) stained with acid ponceau for 5-10 min and rinsed in distilled water three times. Finally, cells were observed under a microscope.

H&E staining

Briefly, the samples were dewaxed and hydrated with gradient alcohol, and the sections were incubated in hematoxylin solution for 15 min followed by washing with PBS. Second, the slices were counterstained with 0.5% eosin solution for 5 min, dehydrated with gradient alcohol, cleared, and sealed. Finally, photos were observed with a light microscope (Keyence, Ōsaka, Japan).

Subcellular fraction

Cells were obtained in PBS and resuspended in 500 μL of ice-cold CLB buffer for 10 min. Homogenization was implemented by applying 15 strokes using a 1 ml needle on ice. Thereafter, 50 μl of 2.5 M sucrose was added to restore isotonic conditions. The first round of centrifugation was implemented at 6300 g for 5 min in a tabletop centrifuge at 4°C. The pellet was washed with TSE buffer at 4000 g for 6 min in a tabletop centrifuge at 4°C until the supernatant was clear. The resulting supernatant was discarded, and the pellets were nuclei. The resulting supernatant from the first round of differential centrifugation was sedimented for 150 min at 14000 rpm in a tabletop centrifuge. The resulting pellets were membranes, and the supernatant was cytoplasmic.

Wound-healing assay

All instruments were sterilized on a clean bench. A marker pen was used to draw a horizontal line 0.5-1 cm from the back of a 6-well plate. At least 5 lines passed through each well. Approximately 5*10^5 cells was added to the plate. The next day, the tip of a pipette was used to make a scratch in a horizontal line. The tip of the pipette was vertical and not inclined. After washing 3 times, serum-free medium was added to a 6-well plate, and we placed the plate into an incubator. Pictures were taken at 0, 6, 12, and 24 h.

Transwell assay

The Transwell membrane was covered with invasion Matrigel. Briefly, the cells were plated on upper chambers with serum-free medium at a density of 5×10^4 cells/well, while the bottom chamber was filled with medium with 10% FBS. After incubation for 24 h, the invaded cells were fixed with ice-cold methanol followed by staining with crystal violet (0.1%). Finally, the cells were observed under a microscope (Olympus, Tokyo, Japan).

Bioinformatic prediction of lncRNA-miRNA interaction

Bioinformatics prediction was performed using the following website: http://starbase.sysu.edu.cn/mirLncRNA.php.

Statistical analysis

All results were presented as means ± SD. The significance between two groups was assessed by unpaired Student's t test or paired t test, and multiple groups were evaluated by one-way ANOVA with Bonferroni post hoc tests. $P<0.05$ was considered significant.

Results

LINC01272 is highly expressed in CD

A total of 60 samples were enrolled in this study; 30 were diagnosed as CD patients, and the others constituted the control group. We collected 2 ml of peripheral blood from the patients and detected LINC01272 expression. The results showed that in patients with CD, the expression of LINC01272 was dramatically higher than that of the control group (**Figure 1A**). Moreover, there was a positive correlation between the levels of LINC01272 in tissue and plasma samples (**Figure 1B**).

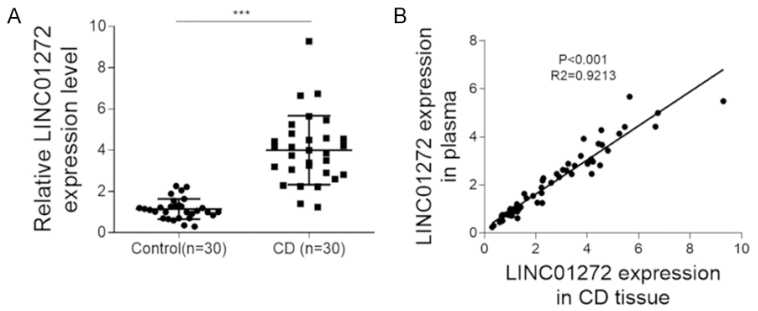

Figure 1. LINC01272 is highly expressed in CD. A. The relative expression of LINC01272 in the control group and CD group. B. Correlation analysis of the expression of LINC01272 in CD tissues and plasma samples. ***P<0.001.

Knockdown of LINC01272 inhibits

TGF-β1-stimulated EMT in IEC-6 cells: Based on the high expression of LINC01272 in CD patients, we speculated that LINC01272 was involved in the development of nonspecific intestinal inflammation. First, TGF-β1 was used to establish an inflammatory cell model, and TGF-β1 significantly promoted the expression of LINC01272 (**Figure 2A**). In addition, sh-LINC01272 and its corresponding control were used to transfect IEC-6 cells. The transfection efficiency is shown in **Figure 2B**, and the results revealed that the expression of LINC01272 was decreased in the sh-LINC01272 group. Next, we investigated the effect of LINC01272 on EMT, the main feature of CD progression, in TGF-β1-treated IEC-6 cells. The mRNA expression of E-cadherin and CK was decreased after TGF-β1 incubation in IEC-6 cells, while knockdown of LINC01272 reversed the effect of TGF-β1 (**Figure 2C**). In addition, TGF-β1 tremendously enhanced the levels of collagen I, collagen II, α-SMA and N-cadherin, which could be arrested by knockdown of LINC01272 (**Figure 2C**). The levels of protein detected by western blot and immunofluorescence presented the same trend as the expression of mRNA (**Figure 2D**, **2E**). Moreover, wound healing and Transwell assays showed that TGF-β1 promoted migration and invasion, which could be prevented by sh-LINC01272 (**Figure 2F**, **2G**). All of these results demonstrated that LINC01272 silencing suppressed TGF-β1-induced EMT in IEC-6 cells.

MiR-153-5p targets the 3'UTR of LINC01272: After subcellular fraction, LINC01272 detected by qPCR was found mainly in the cytoplasm (**Figure 3A**). Through bioinformatics software prediction, we found that miR-153-5p had paired regions targeting the 3'UTR of LINC01272 (**Figure 3B**). Then, a miR-153-5p mimic was used to treat cells, and qRT-PCR assays showed an increase in miR-153-5p in the miR-153-5p mimic group (**Figure 3C**). Luciferase reporter assays showed that the relative luciferase activity was high after pGL3-LINC01272 MUT-Renilla luciferase vector and miR-153-5p mimic cotransfection compared to pGL3-LINC01272 WT-Renilla luciferase vector and miR-153-5p mimic cotransfection, while no significant difference was observed when we replaced the miR-153-5p mimic with NC mimic (**Figure 3D**). RIP assays showed that the relative enrichment of LINC01272 and miR-153-5p bound to Ago2 was high compared with IgG (**Figure 3E**). In addition, the relative expression of miR-153-5p in the blood of CD patients and IEC-6 cells after TGF-β1 treatment was lower than that in the control group (**Figure 3F**, **3G**). Knockdown of LINC01272 enhanced miR-153-5p expression (**Figure 3H**). Pearson's correlation analysis showed that the expression of miR-153-5p was negatively correlated with that of LINC01272 (**Figure 3I**).

LINC01272 regulates TGF-β1-induced EMT through the miR-153-5p axis: To determine whether EMT regulated by LINC01272 was related to miR-153-5p, sh-LINC01272 and miR-153-5p inhibitor were used to transfect TGF-β1-treated IEC-6 cells. As illustrated by the qPCR results, inhibition of miR-153-5p obstructed the positive effect of sh-LINC01272 on the expression of E-cadherin and CK in TGF-β1-treated IEC-6 cells (**Figure 4A**). Moreover, knockdown of miR-153-5p reversed the decrease in collagen I, collagen II, α-SMA and N-cadherin expression caused by sh-LINC01272 in TGF-β1-treated IEC-6 cells (**Figure 4A**). In addition, the expression of protein detected by western blot presented the same trend as the expression of mRNA (**Figure 4B**). Immunofluorescence assays revealed that the low expression of collagen I and collagen II caused by sh-LINC01272 was reversed by the miR-153-5p inhibitor in TGF-β1-treated IEC-6 cells (**Figure 4C**). The wound healing and

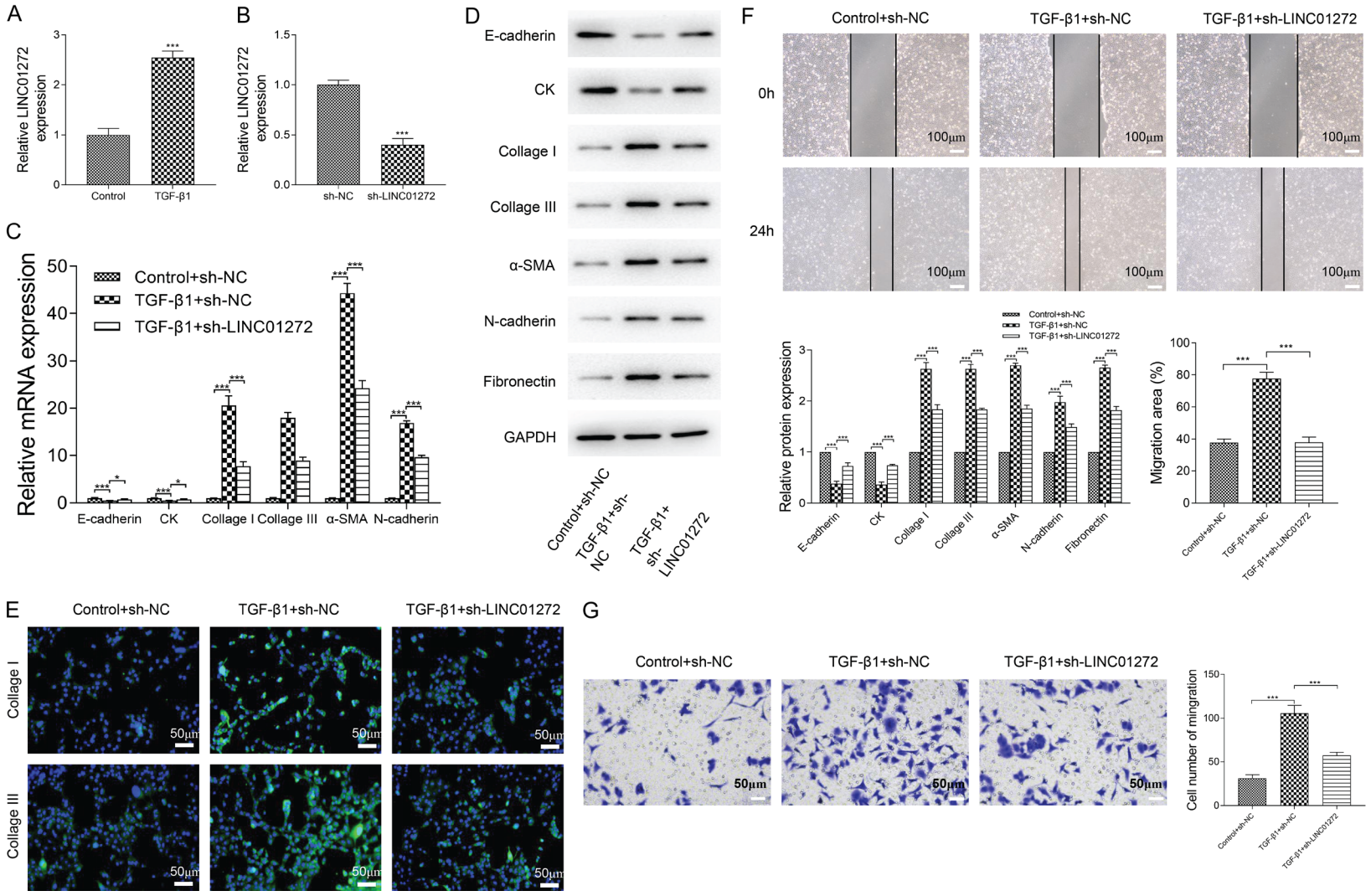

Figure 2. Knockdown of LINC01272 inhibits TGF-β1-induced EMT in IEC-6 cells. A. Relative expression of LINC01272 in TGF-β1-treated IEC-6 cells detected by qRT-PCR. B. The transfection efficiency of sh-LINC01272 detected by qRT-PCR. C. Relative expression of E-cadherin, CK, collagen I, collagen III, α-SMA and N-cadherin mRNA detected by qRT-PCR. D. Expression of E-cadherin, CK, collagen I, collagen III, α-SMA and N-cadherin protein detected by western blot. E. Expression of collagen I and collagen III detected by immunofluorescence. F. Cell migration ability detected by wound-healing assay. G. Cell invasion ability detected by transwell assay. *P<0.05, ***P<0.001.

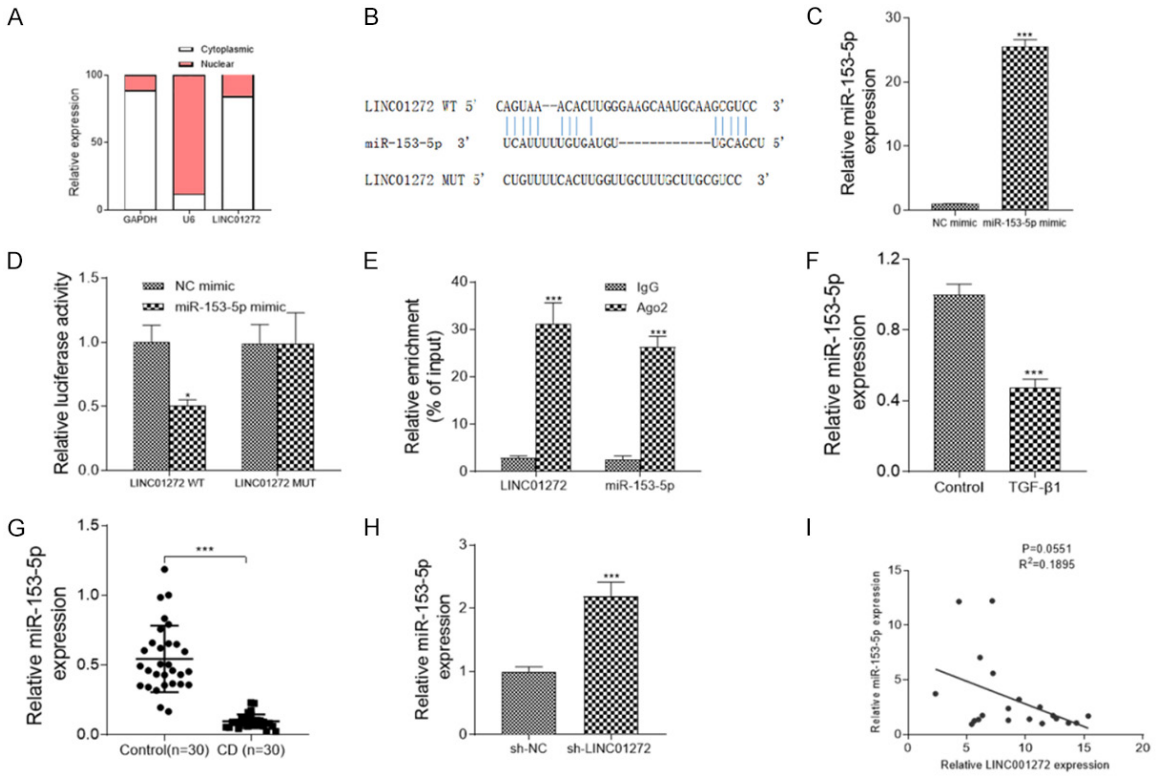

Figure 3. MiR-153-5p targets the 3'UTR of LINC01272. A. Subcellular localization experiment. B. Targeting relationship between LINC01272 and miR-153-3p predicted by bioinformatics. C. The transfection efficiency detected by qRT-PCR. D. A luciferase reporter assay verified the relationship between LINC01272 and miR-153-3p. E. RNA binding protein immunoprecipitation experiments verified the relationship between LINC01272 and miR-153-3p. F. Relative expression of miR-153-3p in TGF-β1-treated IEC-6 cells. G. Relative expression of miR-153-3p in the control group and CD group. H. Relative expression of miR-153-3p before and after silencing LINC01272. I. Pearson's correlation analysis of the relative expression of LINC01272. *P<0.05, ***P<0.001.

Transwell assays showed that sh-LINC01272 inhibited the migratory ability and invasive ability of TGF-β1-treated IEC-6 cells, while inhibition of miR-153-5p rescued the negative influence of sh-LINC01272 (**Figure 4D**, **4E**).

Knockdown of LINC01272 inhibits EMT in CD mice in vivo: We constructed a mouse model by using TNBS and evaluated the DAI score to research the relationship between LINC01272 and EMT *in vivo*. As shown in **Figure 5A**, the DAI score of the TNBS+sh-LINC01272 group dropped over time starting at the 3rd week, while there was no downward trend in the other groups. Histologically, H&E staining showed that the colonic mucosa of the normal control group was intact, and the intestinal glands composed of a single layer of columnar epithelium, lamina propria, and mucosal muscular layer were clearly arranged. In the TNBS group, crypts were destroyed, goblet cells decreased, and epithelial cells were broken. Erosion, ulcer, and inflammatory cell infiltration at various levels of colon tissue were mainly located in the mucosa and submucosa, and most infiltrating cells were lymphocytes and monocytes, that is, the histological changes of chronic colitis. Damaged colon tissue could also be observed in the TNBS+sh-LINC01272 group, but the area and scope and the degree of inflammatory cell infiltration were lighter than those in the TNBS group (**Figure 5B**). In addition, Masson staining showed that in the TNBS group, a large amount of blue-stained collagen could be detected in the submucosa and serosal area, and there was occasional fibrous separation. The colon tissue of mice in the TNBS+sh-LINC01272 group also showed a certain amount of scattered collagen fibers deposited in the above area. However, there were fewer fibers in the TNBS group than in the TNBS group. The normal control group did not demonstrate the above performance (**Figure 5B**). At the protein and mRNA levels, TNBS

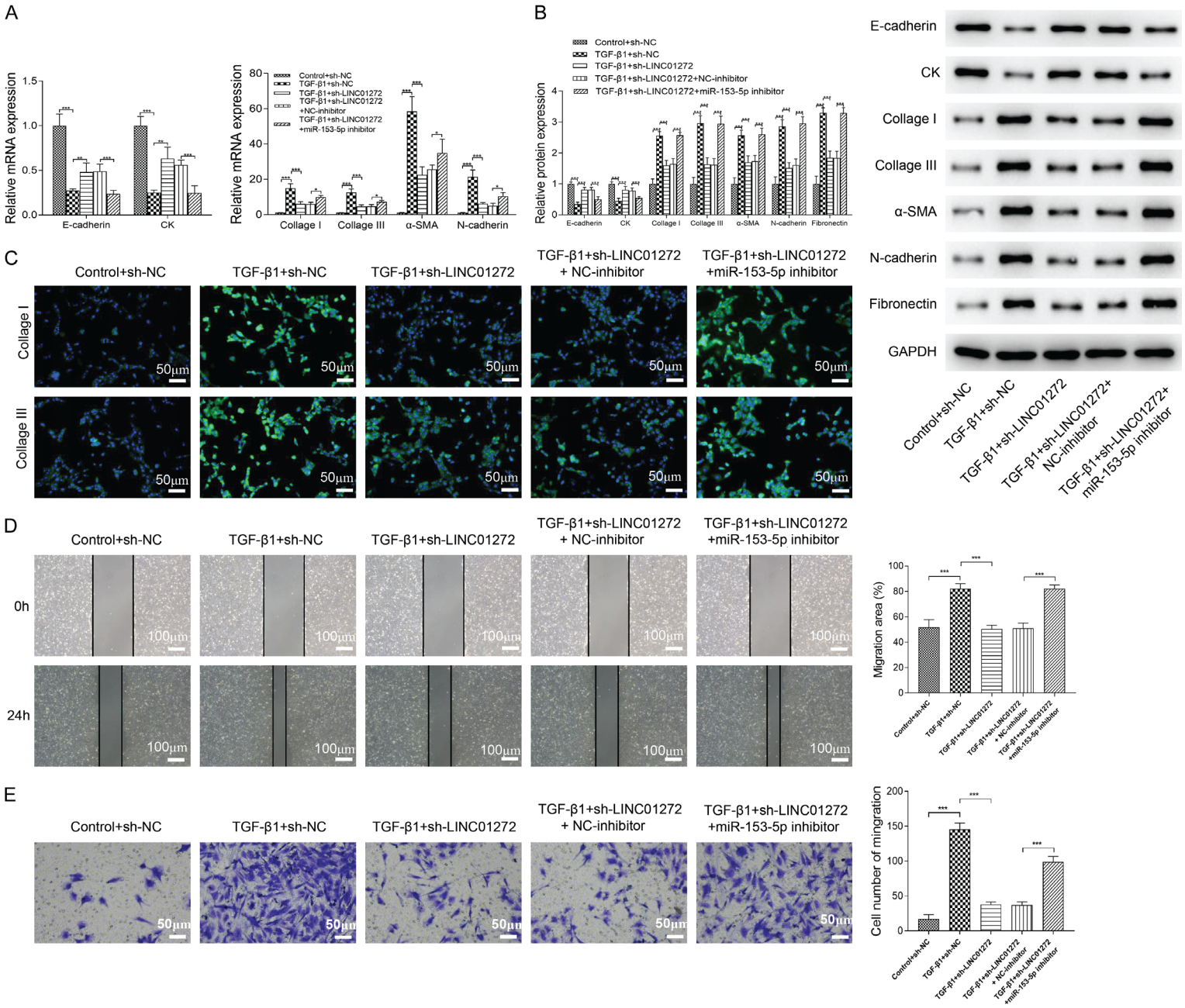
A
Relative mRNA expression
E-cadherin
CK
Relative mRNA expression
Collage I
Collage III
α-SMA
N-cadherin
Control+sh-NC
TGF-β1+sh-NC
TGF-β1+sh-LINC01272
TGF-β1+sh-LINC01272 +NC-inhibitor
TGF-β1+sh-LINC01272 +miR-153-5p inhibitor
B
Relative protein expression
Control+sh-NC
TGF-β1+sh-NC
TGF-β1+sh-LINC01272
TGF-β1+sh-LINC01272+NC-inhibitor
TGF-β1+sh-LINC01272+miR-153-5p inhibitor
E-cadherin
CK
Collage I
Collage III
α-SMA
N-cadherin
Fibronectin
GAPDH
Control+sh-NC
TGF-β1+sh-NC
TGF-β1+sh-LINC01272
TGF-β1+sh-LINC01272+ NC-inhibitor
TGF-β1+sh-LINC01272+ miR-153-5p inhibitor
C
Control+sh-NC
TGF-β1+sh-NC
TGF-β1+sh-LINC01272
TGF-β1+sh-LINC01272 + NC-inhibitor
TGF-β1+sh-LINC01272 +miR-153-5p inhibitor
Collage I
Collage III
50μm
D
Control+sh-NC
TGF-β1+sh-NC
TGF-β1+sh-LINC01272
TGF-β1+sh-LINC01272 + NC-inhibitor
TGF-β1+sh-LINC01272 +miR-153-5p inhibitor
0h
24h
100μm
Migration area (%)
E
Control+sh-NC
TGF-β1+sh-NC
TGF-β1+sh-LINC01272
TGF-β1+sh-LINC01272 + NC-inhibitor
TGF-β1+sh-LINC01272 +miR-153-5p inhibitor
50μm
Cell number of mingration

Figure 4. LINC01272 regulates TGF-β1-induced EMT through the miR-153-5p axis. A. Relative expression of E-cadherin, CK, collagen I, collagen III, α-SMA and N-cadherin mRNA detected by qRT-PCR. B. Expression of E-cadherin, CK, collagen I, collagen III, α-SMA and N-cadherin protein detected by western blot. C. Expression of collagen I and collagen III detected by immunofluorescence. D. Cell migration ability detected by wound-healing assay. E. Cell invasion ability detected by transwell assay. *P<0.05; **P<0.01; ***P<0.001.

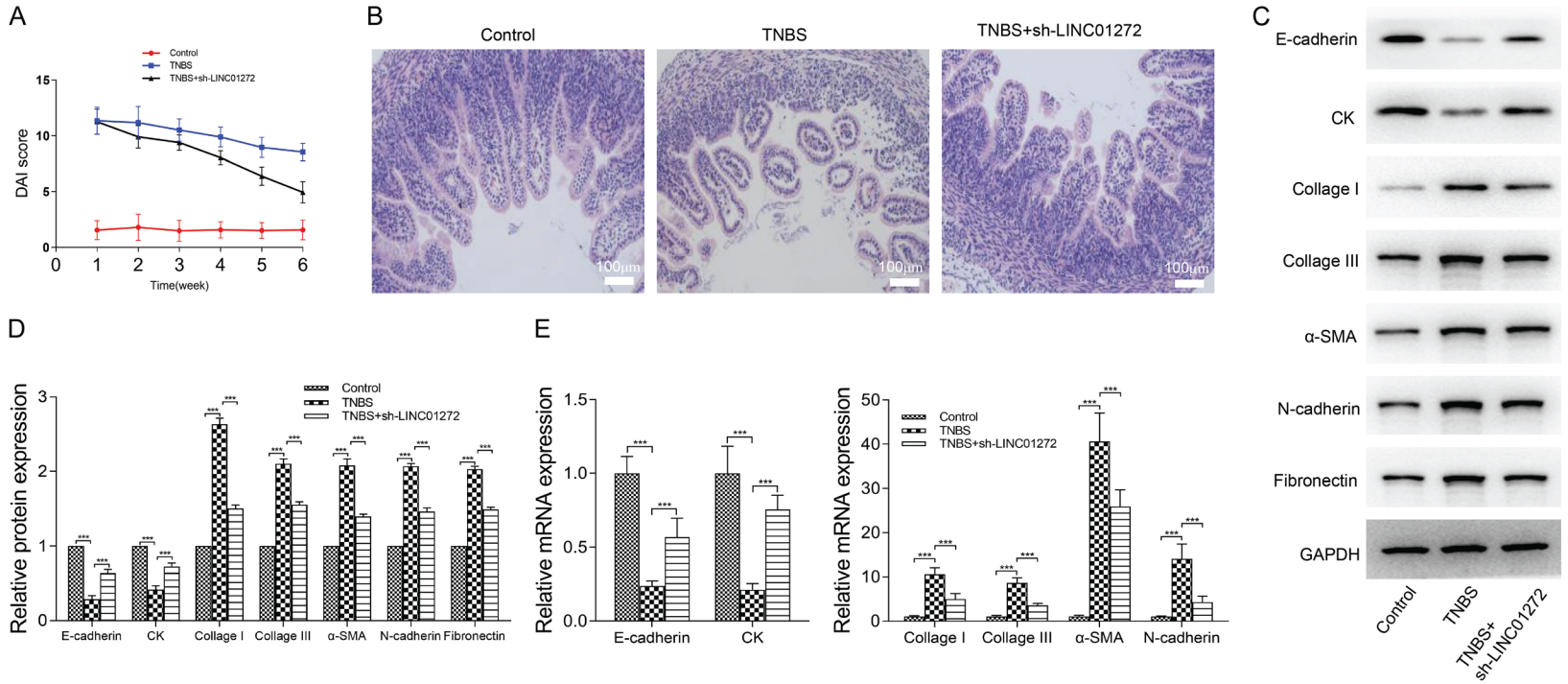

Figure 5. Knockdown of LINC01272 inhibits EMT in CD mice *in vivo*. A. DAI scores of the control group, TNBS group and TNBS+sh-LINC01272 group. B. Pathological manifestations of colon tissue of mice in each group. C, D. Protein levels of EMT-related proteins and fibrosis proteins in each group of mice. E. The mRNA levels of EMT-related proteins and fibrosis proteins in each group of mice. **P<0.01; ***P<0.001.

inhibited E-cadherin and CK expression and promoted collagen I, collagen II, α-SMA and N-cadherin expression, while sh-LINC01272 partly reversed the effects of TNBS (**Figure 5C-E**).

Discussion

Epithelial cell-mesenchymal transition (EMT) is the specific biological process of epithelial cells transforming into cells with a mesenchymal phenotype [27]. It plays an important role in embryonic development, chronic inflammation, tissue remodeling, cancer metastasis and various fibrotic diseases [28]. Through EMT, epithelial cells lose cell polarity and their connection with the basement membrane but acquire mesenchymal phenotypes such as high migration or invasion, anti-apoptosis activity, and the ability to degrade the extracellular matrix. According to biological characteristics and biological markers, the EMT is currently divided into 3 subtypes. Type 1 is related to embryo and organ formation. Type 2 is related to wound healing, tissue regeneration and organ fibrosis. Type 3 is related to tumor progression and metastasis [29]. Many clinical studies have determined that many different organ epithelial cells, such as renal tubules, lens epithelial cells, alveolar epithelial cells, and peritoneal mesothelial cells, are transformed into myofibroblasts and fibroblast phenotypes through EMT, leading to tissue fibrosis [30-32].

Inflammatory bowel diseases include CD and ulcerative colitis. One of the main complications is intestinal stricture caused by fibrosis of the intestinal wall. Intestinal wall fibrosis is due to excessive deposition of extracellular matrix during chronic inflammation and repair of intestinal damage. CD is more likely to produce fibrosis than ulcerative colitis [33]. CD is a chronic nonspecific intestinal disease whose etiology and pathogenesis are unknown thus far. In CD patients, the migration potential of myofibroblasts decreases. Epithelial cell migration, which can be induced by several growth factors, is another sign of intestinal mucosal repair [34]. If fibroblasts cannot cover the damaged tissue, epithelial cells will migrate here. After stimulating effects such as injury, inflammation, and hypoxia, inflammatory and fibrogenic mediators can be activated, which could induce the EMT process. In our study, TGF-β1 was used to induce EMT. After TGF-β1 treatment, the ability to produce large amounts of collagen and fibronectin was achieved, and the migration and penetration capabilities of cells were also changed.

LncRNAs play critical roles in biological processes, such as proliferation, metabolism, differentiation, and apoptosis, whereas altered expression levels contribute to the occurrence of diseases [35]. It was previously reported that LINC01272 accelerates gastric cancer cell migration by EMT [36, 37]. Similarly, we found that the levels of LINC01272 were elevated in CD patients. Furthermore, downregulation of LINC01272 suppressed epithelial cell migration and invasion. Variations in specific markers showed that LINC01272 induced EMT. Therefore, LINC01272 was a potential factor to prevent endothelial migration. Crosstalk between lncRNAs and miRNAs is common in various diseases [38, 39]. MiR-153-5p plays a critical role in LINC01272 regulation of EMT. These data enriched our knowledge of the functionality of miR-153-5p. However, EMT was caused by TGF-β1 *in vitro* or TNBS *in vivo* in this study, and we should further investigate whether the effect of LINC01272 is applicable to EMT caused by other factors, such as genomic variants.

In conclusion, LINC01272 was upregulated, while miRNA-153-5p was downregulated in patients with CD. Our study found that LINC01272 activated EMT through miR-153-5p. This finding contributed to the current understanding of the role of LINC01272 in inflammatory bowel disease and provided a new therapeutic target.

Acknowledgements

This research was supported by a Medical Scientific Research Project of Jiangsu Commission of Health (project number: H2018081) and Science and Technology Development Project of Jiangning District (project number: 2018Ca07).

Disclosure of conflict of interest

None.

Address correspondence to: Wenxia Bai, Gastroenterology, The Affiliated Jiangning Hospital of Nanjing Medical University, Nanjing 211100, Jangsu, China. E-mail: baiwenxia0213@126.com

References

[1] Torres J, Mehandru S, Colombel JF and Peyrin-Biroulet L. Crohn's disease. Lancet 2017; 389: 1741-1755.

[2] Ballester Ferre MP, Bosca-Watts MM and Minguez Perez M. Crohn's disease. Med Clin (Barc) 2018; 151: 26-33.

[3] Harb WJ. Crohn's disease of the colon, rectum, and anus. Surg Clin North Am 2015; 95: 1195-1210.

[4] Chan WPW, Mourad F and Leong RW. Crohn's disease associated strictures. J Gastroenterol Hepatol 2018; 33: 998-1008.

[5] Li J, Mao R, Kurada S, Wang J, Lin S, Chandra J and Rieder F. Pathogenesis of fibrostenosing Crohn's disease. Transl Res 2019; 209: 39-54.

[6] Veauthier B and Hornecker JR. Crohn's disease: diagnosis and management. Am Fam Physician 2018; 98: 661-669.

[7] Schneider SL, Foster K, Patel D and Shwayder T. Cutaneous manifestations of metastatic Crohn's disease. Pediatr Dermatol 2018; 35: 566-574.

[8] Chen Y, Wang Y and Shen J. Role of environmental factors in the pathogenesis of Crohn's disease: a critical review. Int J Colorectal Dis 2019; 34: 2023-2034.

[9] Huang RT, Wang J, Xue S, Qiu XB, Shi HY, Li RG, Qu XK, Yang XX, Liu H, Li N, Li YJ, Xu YJ and Yang YQ. TBX20 loss-of-function mutation responsible for familial tetralogy of Fallot or sporadic persistent truncus arteriosus. Int J Med Sci 2017; 14: 323-332.

[10] Li N and Shi RH. Updated review on immune factors in pathogenesis of Crohn's disease. World J Gastroenterol 2018; 24: 15-22.

[11] Lovisa S, Genovese G and Danese S. Role of epithelial-to-mesenchymal transition in inflammatory bowel disease. J Crohns Colitis 2019; 13: 659-668.

[12] Bataille F, Rohrmeier C, Bates R, Weber A, Rieder F, Brenmoehl J, Strauch U, Farkas S, Furst A, Hofstadter F, Scholmerich J, Herfarth H and Rogler G. Evidence for a role of epithelial mesenchymal transition during pathogenesis of fistulae in Crohn's disease. Inflamm Bowel Dis 2008; 14: 1514-1527.

[13] Kim KK, Kugler MC, Wolters PJ, Robillard L, Galvez MG, Brumwell AN, Sheppard D and Chapman HA. Alveolar epithelial cell mesenchymal transition develops in vivo during pulmonary fibrosis and is regulated by the extracellular matrix. Proc Natl Acad Sci U S A 2006; 103: 13180-13185.

[14] Yu K, Li Q, Shi G and Li N. Involvement of epithelial-mesenchymal transition in liver fibrosis. Saudi J Gastroenterol 2018; 24: 5-11.

[15] Guz M, Dworzanski T, Jeleniewicz W, Cybulski M, Kozicka J, Stepulak A and Celinski K. Elevated miRNA inversely correlates with e-cadherin gene expression in tissue biopsies from Crohn disease patients in contrast to ulcerative colitis patients. Biomed Res Int 2020; 2020: 4250329.

[16] Muise AM, Walters TD, Glowacka WK, Griffiths AM, Ngan BY, Lan H, Xu W, Silverberg MS and Rotin D. Polymorphisms in E-cadherin (CDH1) result in a mis-localised cytoplasmic protein that is associated with Crohn's disease. Gut 2009; 58: 1121-1127.

[17] Cunningham MF, Docherty NG, Burke JP and O'Connell PR. S100A4 expression is increased in stricture fibroblasts from patients with fibrostenosing Crohn's disease and promotes intestinal fibroblast migration. Am J Physiol Gastrointest Liver Physiol 2010; 299: G457-466.

[18] Burke JP, Cunningham MF, Sweeney C, Docherty NG and O'Connell PR. N-cadherin is overexpressed in Crohn's stricture fibroblasts and promotes intestinal fibroblast migration. Inflamm Bowel Dis 2011; 17: 1665-1673.

[19] Yang JX, Rastetter RH and Wilhelm D. Non-coding RNAs: an introduction. Adv Exp Med Biol 2016; 886: 13-32.

[20] Beermann J, Piccoli MT, Viereck J and Thum T. Non-coding RNAs in development and disease: background, mechanisms, and therapeutic approaches. Physiol Rev 2016; 96: 1297-1325.

[21] Fehlmann T, Backes C, Pirritano M, Laufer T, Galata V, Kern F, Kahraman M, Gasparoni G, Ludwig N, Lenhof HP, Gregersen HA, Francke R, Meese E, Simon M and Keller A. The sncRNA zoo: a repository for circulating small noncoding RNAs in animals. Nucleic Acids Res 2019; 47: 4431-4441.

[22] Ambros V. The functions of animal microRNAs. Nature 2004; 431: 350-355.

[23] Zhang X, Hong R, Chen W, Xu M and Wang L. The role of long noncoding RNA in major human disease. Bioorg Chem 2019; 92: 103214.

[24] Paraskevopoulou MD and Hatzigeorgiou AG. Analyzing MiRNA-LncRNA interactions. Methods Mol Biol 2016; 1402: 271-286.

[25] Wang H, Chao K, Ng SC, Bai AH, Yu Q, Yu J, Li M, Cui Y, Chen M, Hu JF and Zhang S. Pro-inflammatory miR-223 mediates the cross-talk between the IL23 pathway and the intestinal barrier in inflammatory bowel disease. Genome Biol 2016; 17: 58.

[26] Spencer DM, Veldman GM, Banerjee S, Willis J and Levine AD. Distinct inflammatory mechanisms mediate early versus late colitis in mice. Gastroenterology 2002; 122: 94-105.

[27] Lee JM, Dedhar S, Kalluri R and Thompson EW. The epithelial-mesenchymal transition: new insights in signaling, development, and disease. J Cell Biol 2006; 172: 973-981.

[28] Radisky DC. Epithelial-mesenchymal transition. J Cell Sci 2005; 118: 4325-4326.
[29] Yang YM and Yang WX. Epithelial-to-mesenchymal transition in the development of endometriosis. Oncotarget 2017; 8: 41679-41689.
[30] Moreno-Amador JL, Tellez N, Marin S, Aloy-Reverte C, Semino C, Nacher M and Montanya E. Epithelial to mesenchymal transition in human endocrine islet cells. PLoS One 2018; 13: e0191104.
[31] Wu C, Ding H, Wang S, Li Y, Liu SB, Wang X, Zheng J, Xue T, Amin HM, Song YH and Zhou J. DAXX inhibits cancer stemness and epithelial-mesenchymal transition in gastric cancer. Br J Cancer 2020; 122: 1477-1485.
[32] Grande MT, Sanchez-Laorden B, Lopez-Blau C, De Frutos CA, Boutet A, Arevalo M, Rowe RG, Weiss SJ, Lopez-Novoa JM and Nieto MA. Snail1-induced partial epithelial-to-mesenchymal transition drives renal fibrosis in mice and can be targeted to reverse established disease. Nat Med 2015; 21: 989-997.
[33] Latella G, Di Gregorio J, Flati V, Rieder F and Lawrance IC. Mechanisms of initiation and progression of intestinal fibrosis in IBD. Scand J Gastroenterol 2015; 50: 53-65.
[34] Stone RC, Pastar I, Ojeh N, Chen V, Liu S, Garzon KI and Tomic-Canic M. Epithelial-mesenchymal transition in tissue repair and fibrosis. Cell Tissue Res 2016; 365: 495-506.
[35] Mirza AH, Berthelsen CH, Seemann SE, Pan X, Frederiksen KS, Vilien M, Gorodkin J and Pociot F. Transcriptomic landscape of lncRNAs in inflammatory bowel disease. Genome Med 2015; 7: 39.
[36] Leng X, Liu G, Wang S, Song J, Zhang W, Zhang X, Rong L, Ma Y and Song F. LINC01272 promotes migration and invasion of gastric cancer cells via EMT. Onco Targets Ther 2020; 13: 3401-3410.
[37] Wang S, Hou Y, Chen W, Wang J, Xie W, Zhang X and Zeng L. KIF9AS1, LINC01272 and DIO3OS lncRNAs as novel biomarkers for inflammatory bowel disease. Mol Med Rep 2018; 17: 2195-2202.
[38] He Z, Yan T, Yuan Y, Yang D and Yang G. miRNAs and lncRNAs in echinococcus and echinococcosis. Int J Mol Sci 2020; 21: 730.
[39] Lai XN, Li J, Tang LB, Chen WT, Zhang L and Xiong LX. MiRNAs and LncRNAs: dual roles in TGF-beta signaling-regulated metastasis in lung cancer. Int J Mol Sci 2020; 21: 1193.